Atomic Spectroscopy

Article

Quantitation and Imaging Analysis of Biological Samples by LA-ICP-MS

Jianzong Zhou,[a] Xin Ni,[a,b] Jiangbin Fu,[a,b] Yatai Li,[a,c] Wei Guo,[a,*] Lanlan Jin,[a] Yue'e Peng,[a,b] and Shenghong Hu[a]

[a] State Key Laboratory of Biogeology and Environmental Geology, China University of Geosciences, Wuhan 430074, P. R. China

[b] Faculty of Materials Science and Chemistry, China University of Geosciences, Wuhan 430074, P. R. China

[c] Key Joint Laboratory of Environmental Simulation and Pollution Control, College of Environmental Science and Engineering, Peking University, Beijing 100871, P. R. China

Received: *April 18, 2021;* ***Revised:*** *May 25, 2021;* ***Accepted:*** *May 25, 2021;* ***Available online:*** *May 27, 2021.*

DOI: 10.46770/AS.2021.068

ABSTRACT: Analysis of the elemental abundance and distribution in biological tissues by laser ablation-inductively coupled plasma mass spectrometry (LA-ICP-MS) adds to clarifying the basic questions of metabolic research and enables bioaccumulation and bioavailability studies in ecological and toxicological risk assessment. In this work, a method based on matrix-matched gelatin calibration LA-ICP-MS for the determination of essential and toxic elements in biological samples was developed. By using a mold-prepared procedure, the elemental inhomogeneity distributions in the synthesized gelatin gels were improved, which was verified by using the 3D (surface- and depth-mapping) LA-ICP-MS protocols. The limits of detection (LODs) ranged from 0.014 μg g^{-1} (Ba) to 48 μg g^{-1} (K). The results of the analysis of biological reference materials (RMs) were in good agreement with the certified values. Furthermore, a reliable bio-mapping LA-ICP-MS method is proposed for studying the metabolism of heavy metals in rat liver injected with CdS/PbS quantum dots. Our results show that the high concentration of Pb and Cd co-exist (positive correlation as high as 78%) in hepatocytes and sinusoids, which indicates that the PbS/CdS quantum dots are not dissociated into toxic heavy metal ions (*i.e.*, Pb^{2+}, Cd^{2+}) in the metabolic process of the liver.

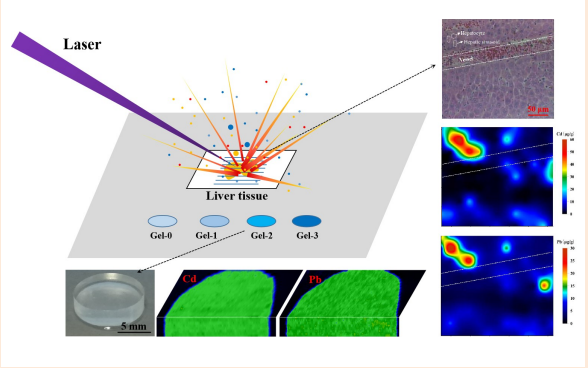

INTRODUCTION

Studying specific elements and their concentrations, distribution, element species or biomolecules in biological tissues is attracting more and more attention in the emerging field of bioanalytics.[1] Many essential elements are involved in innumerable metabolic processes in the biological systems, often functioning as structural components of larger molecules and biocatalysts in diverse biological reactions.[2,3] Quantum dots are frequently used to study the metabolism of organisms. However, quantum dots may also be toxic to tissues, especially when they have decomposed. Understanding the metabolism of quantum dots and its components in tissues is helpful to study the toxic effect of quantum dots on organisms.[4] It is, therefore, vital to understand the abundance and distribution of elements in biological tissues[5].

Laser ablation-inductively coupled plasma mass spectrometry (LA-ICP-MS), as a direct solid sample analytical technique with high spatial resolution (*i.e.* 4~10 μm), has drawn increased interest for elemental quantitative analysis and mapping of biological samples.[6-12] However, the non-stoichiometric effect, also known as the elemental fractionation effect,[13,14] hinders the accurate quantitative analysis of biological samples. Synthesis of biological matrix-matched standards to minimize the fractionation effect [15,16] is used in many laboratories, because there are no commercial solid CRMs available for the majority of biological samples. The conventional method for the synthesis of biological matrix-matched standards involves spiking analytes into similar organic microtome sections and further freezing them.[3,17,18] However, the operation of freezing the microtome section is complex and

homogenization changes the tissue's physical properties, while the cutting processes increase the uncertainty between batches of standards, potentially introducing systematic errors.[19] Besides, standards originating from different tissues have different characteristics. The tedious and complicated preparation and the susceptibility towards systematic errors have encouraged investigation into other standard materials which are easier to manufacture, offer improved traceability and show less variability.

Hydrocolloid gel-based materials are now becoming a promising material for use as the matrix-matched calibration standard for biological samples.[20] In our previous work, spiked agarose gels were used as matrix-matched external standards for conducting quantitative analysis of various food samples.[21] Compared with plant-based food samples, the quantitative results of animal-based samples are obviously poor. The main reason for such problems is that agarose gels are extracted from plants, and the matrix of agarose gels is more similar to plant-based samples. It well-known that the gelatin extracts from animal leather have similar properties as the protein macromolecules and match most animal samples. Therefore, spiked gelatin may be an appropriate calibration standard for animal-based samples.

Gelatin has good solubility, which makes it possible to mitigate the problems associated with homogenates from raw animal tissues.[22-25] However, the obvious phenomenon of element-dependent heterogeneities is found in both gelatin and agarose-gel films. This is caused by the so-called "coffee stain" (visible in the elemental image since higher concentrations are found at the edges) and the "Marangoni" (visible as higher elemental concentrations in the center) effect.[22, 25] The reason for this phenomenon may be that during the drying process, the moisture in the edge area dries quickly, and the internal moisture tends to flow to the edge, resulting in the formation of a concentration gradient.

In this work, we developed a method by which a "mold" is made. and used to form gelatin gels for bio-mapping by LA-ICP-MS analysis. Mold-prepared gelatin forms a more regular shape and flat plane, reducing the influence of the chromatographic effect. After optimization of the prepared conditions of the initial concentration of the gelatin, such as salinity, pH and drying temperature, the elemental homogeneity of the synthesis of the gelatin gels was checked using a 3D LA-ICP-MS protocol. A series of biological powder standard reference materials (SRMs) were used to evaluate the suitability of the gelatin as a matrix-matched external standard. Furthermore, the proposed elemental imaging LA-ICP-MS method was used to investigate the metabolism of the quantum dots in mice liver tissues.

EXPERIMENTAL

Experimentation. Laser sampling was performed using a 193 nm ArF excimer laser ablation system (Geolas 2005, Lambda Physik, Germany), which was coupled to an Agilent 7700x inductively coupled plasma mass spectrometer (ICP-MS, Agilent Technologies, USA). The LA system was warmed up for 30 min before operation and optimization. Helium (0.8 L/min) was used to transport the ablated aerosol from the ablation cell to the ICP-MS, then mixed with argon (0.95 L/min) as the dilution gas before the aerosol was introduced into the plasma. Optimization was conducted by ablating NIST SRM 610 to obtain maximum signal intensity for U^+, while keeping the ThO/Th ratio <0.3% and the U/Th ratio close to 1. The optimized operating parameters for LA-ICP-MS elemental imaging are given in Table 1.

Table 1 LA-ICP-MS Operating Parameters

Laser ablation system	GeoLas HD
Wavelength	193 nm
Energy density	3 J/cm^2
Repetition rate	6 Hz
Spot size	60 μm (Bulk analysis); 32 μm (Imaging)
Line scan speed	32 μm/s
Carrier gas (He) flow rate	0.70 L/min
Makeup gas (Ar) flow rate	0.85 L/min
ICP-MS instrument	**Agilent 7700x**
RF power	1550 W
Auxiliary gas (Ar) flow rate	0.85 L/min
Plasma gas (Ar) flow rate	15 L/min
Dwell time per isotope	10 ms
Measured isotopes	^{23}Na, ^{25}Mg, ^{31}P, ^{39}K, ^{43}Ca, ^{53}Cr, ^{55}Mn, ^{57}Fe, ^{60}Ni, ^{63}Cu, ^{66}Zn, ^{111}Cd, ^{137}Ba, and ^{208}Pb

Reagents and materials. Ultrapure water (18.2 MΩ cm) was used for cleaning the materials and preparing the gelatin standards. A multielement standard solution was prepared from 1000 μg/mL single-element standard solutions purchased from the National Center for Analysis and Testing of Steel Materials (Beijing, P.R. China). Gelatin powder and antifoaming reagent were purchased from Hubei New Universal Chemical Mall (Wuhan, P.R. China). Four biological reference standards (NIST 1566b Oyster tissue, NIST 1577c Bovine liver, GBW08552 Pork powder, GBW08573 Fish meat) were purchased from the National Institute of Standards and Technology (Gaithersburg, MD, USA) and the National Institute of Metrology (Beijing, P.R. China), respectively. After drying for 4 h at 105 °C, the reference standards were placed into a 10-mm diameter mold and pressed at 15 MPa for two minutes to form pellets for the analysis by LA-ICP-MS. The concentration of carbon (as the internal standard) in these standards and the gelatin were determined using the C-S analyzer (CS-900, Beijing Wanlian Dashin Instrument Co. Ltd., P.R. China).

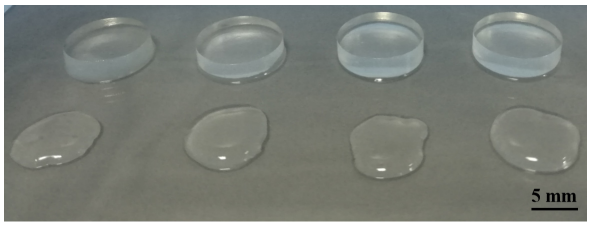

Fig. 1 Photograph of gelatin with (Upper row) and without (Lower row) mold-preparation.

Fig. 2 Spatial distribution of Cd and Pb with and without mold-preparation.

Fig. 3 Relative standard deviation (RSD) of elemental signal in gelatin gels by LA line scanning under different parameters: initial content, pH, solution salinity and temperature. Note: temperature of 10, 20, 30℃ for drying in the oven; 30*、40* ℃ for drying at room temperature.

Preparation of gelatin standards. Gelatin powder was added to the multi-elemental solution and left standing for 30 min at room temperature. Then the fully swollen gelatin was heated in a 60 ℃ ultrasonic bath until the solution was clarified. The hot gelatin solution was transferred to a PVC mold (diameter 12 mm, height 4 mm) and placed on a clean glass pane. After 20 min, the mold was carefully pulled out and the synthetic semi-solid gelatin gels were placed in an oven at 30 ℃ for 3 h to prepare a gelatin film. The final concentrations of the spiked elements in the prepared gelatin samples were validated by using solution nebulization ICP-MS (SN-ICP-MS) after digestion by hydrogen peroxide and nitric acid. In order to verify the homogeneity of the elements in the gelatin samples, we performed 3D element imaging in a gelatin sample by LA-ICP-MS.

Preparation of rat liver tissue. Eight-week-old female C57B/6 rats were purchased from the Wuhan University Animal Experimental Center and housed in a SPF-class animal breeding room. The rats were randomly divided into an experimental group and a control group. The experimental group was injected with 100 μL of PbS/CdS quantum dots in the tail vein, while the control group did not receive any treatment. After 72 h of drug administration, the rats were dissected. After removing the liver, it was fixed with 4% paraformaldehyde for more than 24 h, and was sent to Wuhan Bayer Biotechnology Co., Ltd., for gradient alcohol dehydration and dipping wax packaging. A wax section of 20 μm thickness was cut and subjected to H&E staining. The detailed treatment process can be found in another paper.[17] In addition, multiple indicators of the rats in the experimental group and the control group were measured within 72 h of their arrival at the laboratory.

RESULTS AND DISCUSSION

Characterization of the Gelatin Standards

In the preparation of the multi-elemental gelatin calibration standards, one of the most important difficulties is to achieve homogeneity of the elements in the gelatins. The obvious phenomenon of element-dependent heterogeneities is found in hydrocolloid gel-based films (*i.e.,* gelatin and agarose-gel films). The main reason for the element-dependent heterogeneities both in gelatin and agarose-gel films is due to the different evaporation rates of water in different places when the gel is in the drying and/or forming stage.[22,25] The conventional method is to drop the hot gelatin solution on a slide before drying. Due to the surface tension of the liquid, the gelatin droplets will appear hemispherical, which causes the water evaporation rate at the edge area to accelerate, leading to an increase in elemental concentration. In our experiment, to make the water evaporate evenly and to reduce the concentration gradient of the final gelatin, the hot gelatin solution was put dropwise into a PVC ring with a diameter of 12 mm and a height of 3 mm. After the solution cools naturally, the PVC ring was pulled off. Fig. 1 shows the gelatin both in a mold and without a mold and put directly onto the glass slide. The gelatin in the mold has a regular cylindrical shape and the surface is flat. Because of the surface tension of the liquid, the gelatin without a mold has a circular arc and an irregular edge. Fig. 2 shows the 3D spatial distribution of the spiked elements of Cd and Pb with and without a mold. The elemental signal relative standard deviation (RSD) of the sample in the mold is less than 5%. However, the imaging elemental signal intensity RSD of the gelatin prepared dropwise onto the slide is larger than 10%. The element content in the marginal zone is higher than that in the central zone, especially in the irregular marginal zone. The mold-preparation method makes the water evaporate evenly and reduces the influence of the chromatographic effect to a large extent as well as improves reproducibility.

During the preparation process, we found that the initial contents of the gelatin, solution salinity, pH and drying temperature also affect the final gelatin properties. We also optimized these conditions which may affect the final gelatin properties. Fig. 3 shows the signal relative standard deviation (RSD) of the LA-ICP-MS line scanning on the surface of the gelatin synthesized under different conditions. The initial contents

Fig. 4 Ablation crater of gelatin (a) and the signal of the elements (b).

of the gelatin powder affect the gel film's final thickness and strength. When the initial gelatin powder concentration is too high, the solution will be excessively viscous during the heating and dissolution process, causing the bubbles to stay in the gels and resulting in an uneven distribution of the elements. When the initial gelatin concentration is 12%, a better analysis result can be obtained. The solution pH and its salinity affect the gelatin solubility. The spiked elements were preserved inacidic conditions. The pH and salinity of the gelatin were affected by the amount of added standard solution. When the pH of the gelatin solution was lower than 4 or the salinity higher than 0.2%, insoluble gelatin powder was found in the hot gel solution. This phenomenon may be explained by the fact that high acidity or salinity triggers agarose degradation,[26] which results in an inhomogeneous distribution of the elements in the gelatin. Thus, a pH of 4 and a salinity of 0.2% were selected for preparation of the gelatin standards. In addition, the drying temperature and the drying method may affect the gel's homogeneity due to the temperature gradient on the hot plate and the surrounding air.[22] In this work, the drying temperature used in the oven was 30 ℃ where gelatin shows best homogeneity (Fig. 3).

We also used scanning electron microscopy (SEM) to characterize the ablation behavior of the gelatin samples. As shown in Fig. 4, the LA crater of the gelatin has a regular shape and the elemental signal is stable, which verified the repeatability of the prepared gelatins. The gelatin sample synthesized under the above optimized conditions has strong tenacity and can be stored for more than a week at dry room temperature.

Analytical performance of gelatin standards

In this work, synthesized homogenized gelatins were used as the quantitative calibration standards to measure the elemental concentrations of some biological samples. The analytical performance of the proposed LA-ICP-MS method was evaluated in terms of linearity, limits of detection and accuracy.

The reference concentrations of the elements in the synthesized gelatin standards were confirmed by acid digestion and solution nebulizer ICP-MS (SN-ICP-MS) analysis. As listed in Table 2, most elements in this series of gelatins (Gel-0 is the blank sample, Gel-1, Gel-2, Gel-3 is the spiked elements gelatin.) have a concentration ranging from 1~50 μg/g. Because of the high blank value of the reagents or the gelatin powder used, the concentrations of K, Na, Ca and Mg are difficult to control compared with other elements, the initial concentration determined was taken as the standard value. According to the standard series (Gel-1 to Gel-3), the linear correlation coefficient between the concentration and the analyte signal response was greater than 0.99 for all elements.

When performing quantitative analysis by LA-ICP-MS, the most favorable calibration technique is based on a combination of external standards and internal standards (IS). This strategy was proposed by Longerich *et al.*[27] and has been proven to be the most reliable strategy for obtaining accurate results. The introduction of IS is mainly to correct the variation of the ablation quantity between the different samples. In most biological samples, especially fresh biological samples, water accounts for a large proportion. ^{13}C is prove of an effective IS for calibration of the different ablation and the water quantity.[21,28,29] The IS concentration of carbon in the gelatins and the biological reference materials (NIST 1566b Oyster tissue, NIST 1577c Bovine liver, GBW08552 Pork powder, GBW08573 Fish meat) was determined in advance using the C-S analyzer. The concentration of C in the gelatin gels were 47.51 ± 0.94 %. After a large number of animal-based samples were analyzed for the measurement of

Table 2 The Concentration of Elements in Synthetic Gelatin Standards, μg/g

Elements	Gel-0	Gel-1	Gel-2	Gel-3	Linear equation	R^2
Na	346±19	340±14	351±18	362±21	y=11767x	1
Mg	201±11	214±20	228±11	232±15	y=795x	1
P	428±23	434±26	440±24	437±20	y=489x	1
K	1543±44	1550±41	1564±42	1604±52	y=11896x	1
Ca	68±4	72±5	79±5	132±6	y=21x	1
Cr	0.021±0.001	1.36±0.09	5.66±0.25	54.20±0.45	y=811x-533	0.999
Mn	1.00±0.11	2.38±0.15	8.00±0.18	52.15±0.33	y=16765x-10590	0.9996
Fe	3.66±0.32	5.09±0.45	9.01±0.55	55.24±0.66	y=482x+0.38	1
Ni	0.12±0.01	1.32±0.08	5.68±0.49	51.59±1.05	y=2792x+87	0.9998
Cu	0.21±0.01	2.45±0.09	5.02±0.16	52.85±0.46	y=8259x-1798	1
Zn	0.52±0.03	2.55±0.09	7.21±0.08	56.55±0.18	y=347x-298	0.9988
Cd	0.04±0.01	1.54±0.08	5.52±0.16	50.25±0.29	y=182x-11	0.9999
Ba	0.25±0.02	1.55±0.02	5.33±0.21	48.34±0.27	y=1662x+371	0.9999
Pb	0.04±0.01	1.25±0.04	4.90±0.02	45.36±0.07	y=6878x-1163	0.9997

Table 3 Quantitative Results of Four Biological Samples, μg/g

Elements	LOD	Oyster tissue (NIST 1566b)		Bovine liver (NIST 1577c)		Pork powder (GBW08552)		Fish meat (GBW08573)	
		Determined	Certified	Determined	Certified	Determined	Certified	Determined	Certified
Na	4.25	3021 ± 43	3297 ± 53	1857 ± 20	1950 ± 80	1905 ± 24	2020	1659 ± 23	1706 ± 74
Mg	2.41	1015 ± 18	1085 ± 23	691 ± 14	621 ± 50	1080 ± 23	988 ± 70	1407 ± 28	1320 ± 60
P	14	6324 ± 324	6039 ± 789	12415 ± 378	11750 ± 270	8421 ± 210	8130	8954 ± 311	8514 ± 611
K	48	6687 ± 342	6520 ± 90	11003 ± 440	10230 ± 640	14749 ± 510	14000 ± 310	18010 ± 792	16347 ± 996
Ca	21	868 ± 64	838 ± 20	147 ± 12	131 ± 10	160 ± 14	147 ± 15	531 ± 40	507 ± 100
Cr	0.15	0.420 ± 0.084	-	ND	0.053 ± 0.014	0.345 ± 0.026	0.39	0.364 ± 0.029	0.43
Mn	0.41	17.3 ± 0.5	18.5 ± 0.2	10.0 ± 0.4	10.5 ± 0.5	0.549 ± 0.064	0.48 ± 0.09	0.662± 0.018	0.604 ± 0.108
Fe	2.12	194 ± 12	206 ± 7	187 ± 6	198 ± 0.65	42.8 ± 2.2	43.6 ± 2.4	18.0 ± 0.32	16.7 ± 2.4
Ni	0.02	1.20 ± 0.11	1.04 ± 0.09	0.041 ± 0.013	0.044 ± 0.009	0.093 ± 0.019	-	1.52 ± 0.39	1.5 ± 0.21
Cu	0.42	65.7 ± 1.5	71.6 ± 1.6	301 ± 14	275 ± 4.6	3.97 ± 0.09	3.88 ± 0.15	1.54 ± 0.28	1.36 ± 0.13
Zn	0.57	1469 ± 10	1424 ± 46	172 ± 6	181 ± 1	105 ± 1	94.2 ± 3.6	34.6 ± 2.4	28.8 ± 1.4
Cd	0.024	2.19 ± 0.09	2.48 ± 0.08	0.089 ± 0.010	0.097 ± 0.001	ND	-	ND	0.015
Ba	0.014	9.42 ± 0.20	8.6 ± 0.3	0.031 ± 0.001	-	0.345 ± 0.007	0.39	1.563 ± 0.083	1.75
Pb	0.05	0.351 ± 0.039	0.308 ± 0.009	0.061 ± 0.009	0.063 ± 0.001	0.215 ± 0.075	0.2	0.263 ± 0.023	0.25

"-" No certified value; "ND" Below limits of detection.

their C concentration, we found that the C concentration in animal-based samples is almost the same and on average 46.90 ± 1.70 %. Thus, the average C concentration was used for quantitative calibration. The results of four reference materials by the proposed LA-ICP-MS method are listed in Table 3. The limits of detection (LODs) were calculated from 3 times the standard deviation for 10 replicate measurements of the corresponding analyte signal of a gas blank (helium), as described by Longerich *et al*.[30] The relative sensitivity coefficient of the corresponding analyte was calculated from the calibration curve. The LODs ranged from 0.014 (Ba) to 48 μg g^{-1} (K). As shown in Table 3, the relative errors (REs) between the certified values and the determined values are below 10%, except for some ultra-trace elements (*i.e.,* Cr and Ni). Therefore, the proposed LA-ICP-MS quantitative method, which combines gelatin as the external standards and carbon as IS, could provide a universal approach to the direct analysis of biological samples.

Elemental imaging of rat liver tissue

The proposed LA-ICP-MS method with spiked gelatin gels as the calibration standards was also used to perform elemental imaging analysis. In this work, the elemental distribution in a rat liver tissue injected with CdS/PbS quantum dots was analyzed to examinate the metabolism of heavy metals (Cd and Pb). Fig. 5a shows the Pb and Cd distributions in the areas of distinct blood vessels of rat liver. For the selected imaging area (313 μm × 256 μm), line scan mode was used for imaging analysis (spot size: 32 μm, scanning speed: 32 μm/s) and the total analysis time was 88 s. Totally, 118 data points were obtained in x-axis (laser forward direction) and 9 lines were scanned in y-axis (Fig. 5b).

As shown in Fig. 5c and 5d, a high concentration of Cd and Pb was found in hepatocytes and sinusoids, but were almost completely absent in the blood vessels. Fig. 6 shows the correlation between the Cd and Pb content in rat liver tissue and the Pearson correlation coefficient of the concentration of the two elements was 0.7872. Based on the quantitative imaging results

Fig. 5 Quantitative imaging of Pb and Cd in rat liver tissue. (a) microscopic picture of liver tissue before LA analysis; (b) microscopic picture of liver tissue after LA analysis; (c) Cd quantitative imaging; (d) Pb quantitative imaging.

Fig. 6 Correlation between the Cd content and the Pb content in rat liver tissue.

(Fig. 5 and Fig. 6), it was demonstrated that the PbS/CdS quantum dots did not decompose after metabolism in the liver. Our results match the analysis of the morphology of the quantum dots before injection and in the feces.[4] In routine analysis, the whole organs or tissues of mice need to be taken for acid digestion in order to obtain the element content of the quantum dots, then the metabolism of the quantum dots can be deduced. For the quantum dots composed of multiple elements, the ratio of the elemental concentration after digestion cannot reflect the true distribution in the sample. The proposed LA-ICP-MS quantitative imaging methodology is more direct and, therefore, it is easier to acquire this information. It will also provide important support for further study of the mechanism involved in the toxicity metabolism of a variety of tissues.

CONCLUSIONS

In this work, a gelatin gel was prepared for use as a matrix-matched calibration standard for the analysis of biological samples. Using the mold-prepared method for the synthesis of gelatin achieves better repeatability and a more homogeneous elemental distribution in comparison to the dropwise application onto a slide. The satisfactory quantitative results for biological certified samples were obtained by using the gelatins as the external standard in LA-ICP-MS analysis. A reliable bio-mapping LA-ICP-MS method is proposed for determining the metabolism of heavy metals in rat liver injected with CdS/PbS quantum dots. Our results show that the high concentration of Pb and Cd co-exist (positive correlation as high as 78%) in hepatocytes and sinusoids, which indicates that the PbS/CdS quantum dots are not dissociated into toxic heavy metal ions (*i.e.,* Pb^{2+}, Cd^{2+}) in the metabolic process of the liver.

AUTHOR INFORMATION

Corresponding Author

* W. Guo

Email address: wei.guo@cug.edu.cn

Notes

The authors declare no competing financial interest.

ACKNOWLEDGMENTS

This work was supported by the National Natural Science Foundation of China (41873072, 41521001, and 4202010400), the Fundamental Research Funds for the Central Universities (CUG170102 and CUG180603).

REFERENCES

1. I. Konz, B. Fernandez, M. L. Fernandez, R. Pereiro, and A. Sanz-Medel, *Anal. Bioanal. Chem.*, 2012, **403**, 2113-2125. https://doi.org/10.1007/s00216-012-6023-6
2. A. Hanć, I. Komorowicz, M. Iskra, W. Majewski and D. Barałkiewicz, *Anal. Bioanal. Chem.*, 2011, **399**, 3221-3231. https://doi.org/10.1007/s00216-011-4729-5
3. D. J. Hare, E. P. Raven, B. R. Roberts, M. Bogeski, S. D. Portbury, C. A. McLean, C. L. Masters, J. R. Connor, A. I. Bush, and P. J. Crouch, *NeuroImage*, 2016, **137**, 124-131. https://doi.org/10.1016/j.neuroimage.2016.05.057
4. M. Zhang, J. Yue, R. Cui, Z. Ma, H. Wan, F. Wang, S. Zhu, Y. Zhou, Y. Kuang, and Y. Zhong, *Proc. Natl. Acad. Sci. U.S.A*, 2018, **115**, 6590-6595. https://doi.org/10.1073/pnas.1806153115
5. T. Jin and Y. Imamura, *ECS J. Solid State Sci. Technol.*, 2015, **5**, R3138-R3145. https://doi.org/10.1149/2.0171601jss
6. B. Chen, J. T. Lum, Y. Huang, B. Hu, and K. S. Leung, *Anal. Chim. Acta*, 2019, **1082**, 18-29. https://doi.org/10.1016/j.aca.2019.07.044
7. B. Neumann, S. Hosl, K. Schwab, F. Theuring, and N. Jakubowski, *J. Neurosci. Meth.*, 2020, **334**, 108591. https://doi.org/10.1016/j.jneumeth.2020.108591
8. I. Moraleja, M. L. Mena, A. Lazaro, B. Neumann, A. Tejedor, N. Jakubowski, M. M. Gomez-Gomez, and D. Esteban-Fernandez, *Talanta*, 2018, **178**, 166-171. https://doi.org/10.1016/j.talanta.2017.09.031
9. C. Ishii, S. M. M. Nakayama, A. Kataba, Y. Ikenaka, K. Saito, Y. Watanabe, Y. Makino, T. Matsukawa, A. Kubota, K. Yokoyama, H. Mizukawa, T. Hirata, and M. Ishizuka, *Chemosphere*, 2018, **212**, 994-1001. https://doi.org/10.1016/j.chemosphere.2018.08.149
10. O. Hachmoller, M. Aichler, K. Schwamborn, L. Lutz, M. Werner, M. Sperling, A. Walch, and U. Karst, *J. Trace Elem. Med. Biol.*, 2016, **35**, 97-102. https://doi.org/10.1016/j.jtemb.2016.02.001
11. M. R. Flórez, M. Aramendía, M. Resano, A. C. Lapeña, L. Balcaen, and F. Vanhaecke, *J. Anal. At. Spectrom.*, 2013, **28**, 1005-1015. https://doi.org/10.1039/c3ja50087j
12. D. J. Hare, E. P. Raven, B. R. Roberts, M. Bogeski, S. D. Portbury, C. A. McLean, C. L. Masters, J. R. Connor, A. I. Bush, P. J. Crouch, and P. A. Doble, *Neuroimage*, 2016, **137**, 124-131. https://doi.org/10.1016/j.neuroimage.2016.05.057
13. B. Fernández, F. Claverie, C. Pécheyran, O. F. X. Donard and F. Claverie, *TrAC-Trend. Anal. Chem.*, 2007, **26**, 951-966. https://doi.org/10.1016/j.trac.2007.08.008
14. F. Claverie, B. Fernández, C. Pécheyran, J. Alexis, and O. F. X. Donard, *J. Anal. At. Spectrom.*, 2009, **24**, 849-988. https://doi.org/10.1039/b904134f
15. D. Pozebon, G. L. Scheffler, and V. L. Dressler, *J. Anal. At. Spectrom.*, 2017, **32**, 890-919. https://doi.org/10.1039/c7ja00026j
16. D. Hare, C. Austin, and P. Doble, *Analyst*, 2012, **137**, 1527-1537. https://doi.org/10.1039/c2an15792f
17. A. Matusch, L. S. Fenn, C. Depboylu, M. Klietz, S. Strohmer, J. A. McLean and J. S. Becker, *Anal. Chem.*, 2012, **84**, 3170-3178. https://doi.org/10.1021/ac203112c
18. A. Kindness, C. N. Sekaran, and J. Feldmann, *Clin. Chem.*, 2003, **49**, 1916-1923. https://doi.org/10.1373/clinchem.2003.022046
19. K. A. Dorph-Petersen, J. R. Nyengaard, and H. J. G. Gundersen, *J. Microsc.*, 2010, **204**, 232-246. https://doi.org/10.1046/j.1365-2818.2001.00958.x
20. H. J. Stärk and R. Wennrich, *Anal. Bioanal. Chem.*, 2011, **399**, 2211-2217. https://doi.org/10.1007/s00216-010-4413-1

21. Y. Li, W. Guo, Z. Hu, L. Jin, S. Hu, and Q. Guo, *J. Agric. Food. Chem.*, 2019, **67**, 935-942. https://doi.org/10.1021/acs.jafc.8b05479
22. M. Šala, V. S. Šelih, and J. T. van Elteren, *Analyst*, 2017, **142**, 3356-3359. https://doi.org/10.1039/c7an01361b
23. R. Niehaus, M. Sperling and U. Karst, *J. Anal. At. Spectrom.*, 2015, **30**, 2056-2065. https://doi.org/10.1039/c5ja00221d
24. A. C. Niehoff, J. Grünebaum, A. Moosmann, D. Mulac, J. Söbbing, R. Niehaus, R. Buchholz, S. Kröger, A. Wiehe, and S. Wagner, *Anal. Chim. Acta*, 2016, **938**, 106-113. https://doi.org/10.1016/j.aca.2016.07.021
25. H. Sela, Z. Karpas, H. Cohen, Y. Zakon, and Y. Zeiri, *Int. J. Mass Spectrom.*, 2011, **307**, 142-148. https://doi.org/10.1016/j.ijms.2011.01.022
26. M. H. Norziah, S. L. Foo and A. A. Karim, *Food Hydrocolloid.*, 2006, **20**, 204-217. https://doi.org/10.1016/j.foodhyd.2005.03.020
27. H. P. Longerich, S. E. Jackson, and D. Günther, *J. Anal. At. Spectrom.*, 1996, **11**, 899-904. https://doi.org/10.1039/ja9961100899
28. J. Chirinos, D. Oropeza, J. Gonzalez, V. Zorba, and R. E. Russo, *Appl. Spectrosc.*, 2017, **71**, 709-720. https://doi.org/10.1177/0003702816683686
29. D. A. Frick and D. Günther, *J. Anal. At. Spectrom.*, 2012, **27**, 1294-1303. https://doi.org/10.1039/c2ja30072a
30. H. P. Longerich, S. E. Jackson, and D. Günther, *J. Anal. At. Spectrom.*, 1996, **12**, 391-391. https://doi.org/10.1039/ja9961100899